frontiers in Energy Research

ORIGINAL RESEARCH
published: 16 July 2020
doi: 10.3389/fenrg.2020.00138

Impact of Biomass Source and Pyrolysis Parameters on Physicochemical Properties of Biochar Manufactured for Innovative Applications

*Ana Uroić Štefanko and Danuta Leszczynska**

Department of Civil and Environmental Engineering, Jackson State University, Jackson, MS, United States

Manufacturing biochar for energy and high-tech applications requires a specific set of physicochemical parameters based on relationships between initial pyrolytic conditions and properties of starting material, namely biomass. This study compares 20 types of biochar produced from five diverse waste biomasses at two pyrolytic temperatures (400, 700°C), processing times (2, 5 h) and heating rates (26, 5°C/min). The manufactured biochar was tested for the yield, fixed C, ash load, size of developed surface area, porosity, nutrients, and minerals. Leachate tests were performed to determine the stability of biochar, their pH, conductivity, and presence of dissolved nutrients and metals. The proximate analysis demonstrated an increase in fixed C linked to temperature increase from 400 to 700°C. Biochar produced from organic-rich biomass such as corn stover showed higher content of nutrients, especially potassium and phosphorus on their surfaces and in their leachates, which influenced the development of its surface area at 700°C. The increase of temperature with prolonged residence time has generated more stable and mostly aromatic structures within biochar when compared to other studied conditions. These findings were confirmed by the FTIR spectra that indicated amplified condensation of aromatic and aliphatic carbons (C = C, C = O, C-H) and a decrease of phenolic bonded water (-OH bonded). Consequently, a specific application of biochar should ultimately dictate the choice of optimal pyrolytic conditions linked to the components of initial biomass.

Keywords: pyrolysis, organic-rich waste biomass, biochar, functional groups, leachate, SEM, FTIR

OPEN ACCESS

Edited by:
Wei-Yin Chen,
University of Mississippi, United States

Reviewed by:
Halil Durak,
Yüzüncü Yil University, Turkey
Mengxiang Fang,
Zhejiang University, China

****Correspondence:***
Danuta Leszczynska
danuta.leszczynska@jsums.edu

Specialty section:
This article was submitted to Bioenergy and Biofuels, a section of the journal Frontiers in Energy Research

Received: *03 February 2020*
Accepted: *04 June 2020*
Published: *16 July 2020*

Citation:
Uroić Štefanko A and Leszczynska D (2020) Impact of Biomass Source and Pyrolysis Parameters on Physicochemical Properties of Biochar Manufactured for Innovative Applications. Front. Energy Res. 8:138. doi: 10.3389/fenrg.2020.00138

INTRODUCTION

In current years, biochar-oriented research has shifted from the agricultural use to high-tech applications, and now it is more focused on the targeted development of physicochemical properties required for specific non-agricultural technologies. Already published results indicate that the successful production for the custom-made use should require a comprehensive study of the range of pyrolytic conditions applied to the variety of initial biomasses.

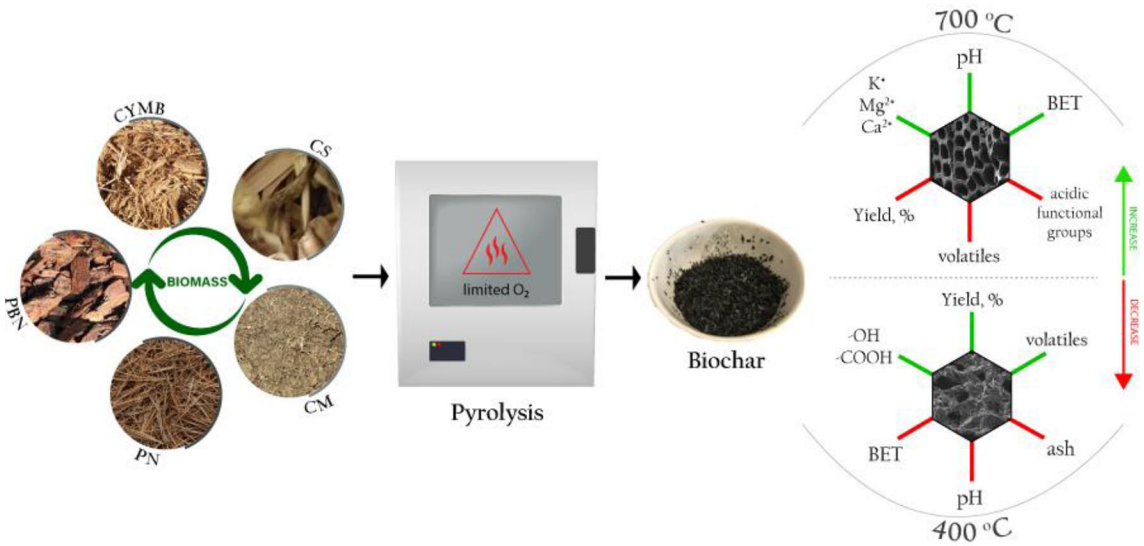

GRAPHICAL ABSTRACT

For example, Mohanty et al. (2018) reported that the increase of pyrolytic temperature would promote volatilization with the formation of pores, as one way to modify biochar's surface. The optimization of residence time and the heating rate would play a crucial role in obtaining anticipated surface alterations that occur during pyrolysis. On the other hand, the altered surface area with controlled porosity and excess of surface-bound functional groups denote how adaptable the use of biochar could be in a respect to pyrolytic conditions of initial biomass (Ahmad et al., 2014; Rajapaksha et al., 2016; Mohanty et al., 2018).

Generally, the initial ratio of three main structural components, namely cellulose, hemicellulose, and lignin will dictate the rate and mechanisms of biomass degradation. Although many proposed mechanisms facilitate the prediction on how to obtain favorable properties, other literature contradicts the clarity of initial reactions (Mayes and Broadbelt, 2012). Accordingly, experimental results in many studies often agree and disagree to what extent a certain pyrolytic parameter affects biochar properties. In a study conducted by Durak et al. (2019), the influence of catalyst on the product content and yield has shown to be significant for the high conversion rates [78.91% (Al2O3) and 76.06% (SnCl4·5H2O)], while high heating values (HHV) of liquid products were reported higher without the addition of a catalyst. In other studies, a negative effect was observed as the addition of catalyst decreased liquid, solid, or gas yield (Yorgun and Simşek, 2008; Durak, 2016). Considering different reaction pathways that biomass could potentially undergo (Kawamoto et al., 2003; Patwardhan et al., 2011; Lv and Wu, 2012; Kawamoto, 2017; Durak et al., 2019), disparities among researchers in fundamental observance of biomass decomposition suggests a need for a more improved systematic characterization. As a result, only a comprehensive understanding of the linkage between process parameters and biomass precursors can contribute to the fine-tuning of biochar properties.

According to Fahmi et al. (2018), a low initial pyrolytic temperature (<500°C) could produce biochar with a more significant number of functional groups, higher cation exchange capacity (CEC) and enhanced yield. Conversely, due to insufficient thermal degradation, such biochar would often have small surface area caused by the structural stability of lignocellulosic molecules and volatiles at lower temperatures (Uchimiya et al., 2011). When biochar was produced at higher pyrolytic temperatures, it exhibited greater surface areas due to the volatilization of different fractions of biomass with simultaneous expansion of micropores (Chen et al., 2008). In addition, the increase and/or decrease of pyrolytic temperature might influence the final pH (Fahmi et al., 2018).

While exhibited properties could define biochar potential applications, there are still numerous obstacles that could cause practical drawbacks. For example, while electrical conductivity and ash content are beneficial properties for agricultural use, novel energy applications of biochar would consider increased mineral content as an impurity (Ngan et al., 2019). On the contrary, increased thermal treatment (>900°C) could increase biochar carbonization >90% (wt.) and conductivity, while decreasing ash content. In a study conducted by Gabhi et al. (2017), the high thermal treatment (950°C) of maple-wood biochar resulted in increased electrical conductivity, achieving higher skeletal conductivity (343.2 S/m) in comparison to a single graphite crystal (333.3 S/m). This important observation leads to the discovery of a new phenomenon called "elastic behavior of electrical conductivity."

Furthermore, the environmental application of biochar generally inclines toward the production of an extensive surface and abundance of functional groups, such as hydroxyl, carboxyl, and phenolic for successful removal of contaminants from water.

Much research has been conducted and validated a positive effect of functional groups on the increased adsorption of heavy metals (Cao et al., 2009; Lu et al., 2012; Ngan et al., 2019). For example, Mohanty et al. (2018) reported that heavy metals could be removed from the water matrix due to the metal-binding on negatively charged biochar's surface formed through the reduction of pyrolysis' temperature (Mukherjee et al., 2011; Suliman et al., 2017). As a result, a type of aliphatic or aromatic surface could be determined based on the dissociation of different carboxyl moieties (Harvey et al., 2012). Moreover, biochar's surface charge and the electrostatic interaction between ions, nanoparticles, and active biochar surface is strongly coordinated by changes in pH (Wang et al., 2013; Xiao et al., 2018). Apart from being observed as a direct binding site for pollutants, functional groups are also extensively researched to serve as active sites for enhanced modification via oxidation (Xue et al., 2012), sulfonation (Kastner et al., 2012) and amination (Yang and Jiang, 2014).

Generally, targeted removal of a specific contaminant could be governed by adsorbent-adsorbate interactions through combined adsorption/ion exchange mechanisms. Uchimiya et al. (2011) reported that the governing mechanism could be a function of variating dimensions of pores, thus contributing to greater ion exchange. Lu et al. (2012) and Cao et al. (2009) additionally explained the benefits of nutrient-rich biochar, which could enhance complexation and formation of precipitates in reactions with metallic contaminants, thus additionally increasing the overall removal efficiency. The inorganic phase in biochar can undergo many different reactions of which chloridized, hydroxylated, or carbonated metals are of special interest. With the increase of pyrolytic temperature, they transition to metallic oxides, of which some can reduce to pure metals (Xiao et al., 2018). Taking advantage of such a process occurring in a limited oxygen environment, successful magnetic (Chen et al., 2011) and zerovalent Fe (Yan et al., 2015) biochar have also been synthesized. In accordance, characterization of initial biomass and its pyrolytic conditions proves to be crucial in defining beneficial properties of obtained types of biochar and in assessing their role toward diverse applications.

There is a growing trend in studying biochar toward environmental clean-up and energy-saving applications. Published results point out that the contrary to environmental benefits, biochar might also have an adverse effect due to possible leaching of toxic metals that are part of biochar. The ultimate development of physicochemical properties responsible for the efficiency without detrimental effects would be directly related to the optimal pyrolytic conditions of cautiously chosen initial biomass (Ahmad et al., 2012; Gai et al., 2014; Mohan et al., 2014).

The main objective of this study was to establish correlations between initial pyrolytic conditions of various types of biomass and the formation of favorable properties of produced biochar toward potential replacement of more expensive carbon-based nanomaterials or to be used as *in situ* adsorber. To achieve this goal, 20 different types of biochar were manufactured in pre-set conditions from five types of organic waste biomass. Obtained biochars were extensively tested for their organic and inorganic content, surface formation and size, the existence of functional groups, possible leachability, and stability in various conditions.

MATERIALS AND METHODS

Biomass Selection and Pretreatment

Five types of biomass obtained locally in Mississippi, USA, were selected to produce a total of 20 types of biochar. The selection of biomass represents a variety of organic waste biomass that is abundant locally and could be a potential source for the centered biochar production. In addition, the rich agricultural and horticultural sector that holds a great part of the Mississippi State's economy could benefit economically from the targeted production of biochar for non-agricultural purposes. While most State's farms focus on livestock and dairy produce, Mississippi is also known as one of the country's top producers of wood-related products.

Pine bark nuggets (PBN) and cypress mulch blend (CYMB) were collected from a local company manufacturing landscaping material in Brookhaven; pine needles (PN) were collected in a large homogenous batch from Byram; cow manure (CM) was collected from a small farm in Canton, and corn stover (CS) was collected in a larger batch from different locations around Mississippi. Each biomass was placed under the fume hood for 48 h prior pyrolysis to remove the moisture from raw material. After drying, the biomass was pulverized to a particle size of 1–2 cm and stored in sealed containers.

Biomass Pyrolysis

Biochar pyrolysis was completed in two types of bench-top furnaces under two settings of initial conditions. The first batch of 10 types of biochar was produced in a muffle furnace (1,400 Thermolyne, Thermo Fisher Scientific, USA) at two temperatures (400°C and 700°C) with a fixed heating rate of 26°C/min for 2 h. The second batch of the remaining 10 types of biochar was produced in a programmable furnace (StableTemp Furnace, Cole-Parmer, USA) at the same two temperatures of 400 and 700°C with a lower heating rate of 5°C/min for 5 h. A stainless-steel vessel with a cover was employed to minimize oxidation occurring in a limited oxygen environment. Approximately 200 g of biomass was used to produce each biochar, and the obtained yield was calculated using the following Equation (1) (Narzari et al., 2017):

$$Biochar\ yield\ (\%) = \frac{W_f}{W_i} x\ 100 \quad (1)$$

where W_f = mass (g) after pyrolysis; W_i = mass (g) before pyrolysis.

To distinguish between different types of biochar, they were denoted with the appropriate abbreviations followed by the pyrolytic temperature (400 and 700°C) and residence time (2 or 5 h), such as XX400-2, XX700-2, XX400-5, and XX700-5.

Proximate Analysis

The determination of moisture, ash, volatile, and fixed carbon has followed an adaptation of the ASTM-D1762-84 method distinctively improved for biochar (Singh et al., 2017). Prior

analysis, all biochar samples were sieved to obtain a particle size of 0.25–0.50 mm. Crucibles were pre-fired for 6 h at 750°C and then cooled to 105°C to reduce any volatile residuals. For the determination of moisture, biochar was heated in covered crucibles for 18 h at 105°C. The volatile matter was determined by heating biochar in covered crucibles for 10 min in a pre-heated furnace at 950°C. Ash content was obtained by heating biochar in crucibles with covers askew for 6 h at750°C.

About one gram (1 g) of each biochar was used for proximate analysis. All tests were repeated twice and averaged. Moisture, volatile, ash, and fixed carbon content were calculated as follow (Singh et al., 2017):

$$Moisture\ (\%) = \frac{W_{as\ received} - W_{105\ ^\circ C\ dried}}{W_{as\ received}}\ 100 \quad (2)$$

$$Volatile\ matter\ (\%) = \frac{W_{105\ ^\circ C\ dried} - W_{950\ ^\circ C\ devolatilised}}{W_{105\ ^\circ C\ dried}} x\ 100 \quad (3)$$

$$Ash\ (\%) = \frac{W_{residue\ after\ 750\ ^\circ C}}{W_{105\ ^\circ C\ dried}} x\ 100 \quad (4)$$

$$Fixed\ carbon\ (\%) = \frac{W_{105\ ^\circ C\ dried} - W_{950\ ^\circ C\ devolatilised} - W_{residue\ after\ 750\ ^\circ C}}{W_{105\ ^\circ C\ dried}} x\ 100 \quad (5)$$

Where: W = mass (g) of biochar.

pH and Conductivity (EC) Measurements

pH and conductivity were measured in the leachate prepared as described below. Biochar placed in a 50 ml test tube and mixed well with deionized water (DIW) in a ratio of 1:20 (0.5 g biochar:10 ml DIW) was shaken for 1 h at 25°C and allowed to stand for 30 min before the measurement. pH was determined using the pH meter (Mettler Toledo, USA), and conductivity by the conductivity meter (Oakton Instruments, USA).

BET (Brunauer-Emmett-Teller) Surface Area

Determination of biochar's surface area, an average pore's volume, and the average pore's sizes were performed with the adsorption of nitrogen (N_2) at 77 K using the Brunauer-Emmett-Teller (BET) method (Brunauer et al., 1938). The analysis was achieved using the TriStar II Plus analyzer (Micromeritics, USA). This method is based on the adsorption and desorption volumes of nitrogen gas under different relative pressures. BET reports were obtained via MicroActive v. 2.03 software. Prior analysis, each biochar sample was degassed for 2 h at 100°C.

FTIR (Fourier-Transform Infrared Spectroscopy)

FTIR images were collected with Spectrum Two (PerkinElmer, Inc., MA, USA) with the $LiTaO_3$ (lithium tantalate) MIR detector and standard optical system with a KBr window. The obtained data represents results over the spectral range of 400–4,000 cm^{-1}. No special preparation of biochar was needed; the sample was directly placed on the KBr window for analysis, and the readings were obtained through the Spectrum Two software.

SEM-EDX Analysis

The morphology of biochar structures was determined with SEM images with the scanning electron microscope (SEM) model TESCAN LYRA3 FIB-SEM (TESCAN, Brno, CZ). The SEM images were taken under different acceleration voltages (kV) and magnifications (μm) to emphasize morphological changes in studied biochar. Electron Dispersive X-Ray (EDX) spectral analysis investigated all corresponding elements (nutrients and metals) in each sample. Specimens of biochar were mounted on the aluminum pin with carbon conductive glue and placed for analysis. SEM imaging and EDX analysis were obtained with the TESCAN image processing software.

Biochar Leachate Analysis for Nutrients and Metals

Nutrients and metal constituents within biochar were determined with the inductively coupled plasma emission spectrometer (ICPE) Shimadzu ICPE-9,000 (Shimadzu, Japan). Biochar samples were mechanically shaken in deionized water for 1 h (0.5 g biochar:10 ml DIW). The solution was allowed to settle for 30 min. Prior analysis, the solution was vacuum-filtered through a Whatman (0.45 μm) glass membrane filter and acidified with a concentrated HNO_3 (Fisher Scientific, USA). Obtained results were reported as mg/kg and g/kg.

RESULTS AND DISCUSSION

Biochar Yield and Proximate Analysis

Biochar pyrolysis carried under pre-set conditions (biomass type, pyrolytic temperature, residence time, and heating rate), resulted in the production of 20 kinds of biochar with various physicochemical characteristics. Controlled pyrolysis of biomasses yielded a variation of biochar's masses depending on the choice of pyrolytic temperature (400, 700°C), residence time (2, 5 h) and heating rate (5, 26°C/min).

As presented in **Table 1**, biochar's yield ranged from 26.1% (cypress mulch blend, CYMB, 700°C) to 60.8% (pine bark nuggets, PBN, 400°C) and substantially decreased when the higher pyrolytic temperature was applied. The same trend was observed for all types of biochar, which confirmed more significant thermal decomposition of volatiles with a lower molecular weight at a pyrolytic temperature of 700°C. Moreover, a limited structural aromatization of aliphatic molecules occurred at higher temperatures as well, which was aligned with Zhang et al. (2015) findings.

Interestingly, all pine bark nuggets (PBN) types of biochar had the highest yield with the highest carbon content. Our yields were more than 50% higher than the yields reported by Park et al. (2019), who employed similar pyrolytic conditions, but under the nitrogen gas only. It should be noted that our pyrolytic tests were done under limited oxygen presence and without initial purge with nitrogen gas but provided a better yield of the final product. In contrast, cypress mulch blend made (CYMB) biochar showed the lowest yield independently from the initial pyrolytic

TABLE 1 | Proximate analysis of corn pine nuggets (PBN), corn stover (CS), pine needle (PN), cow manure (CM), and cypress mulch barks (CYMB) made biochars produced under different pyrolytic conditions.

Biochar	Temp., °C	Residence time, h/Heating rate°C/min	Yield, %	Moisture[a], %	Ash[a], %	Volatile[a], %	Fixed C[a], %
PBN400-2	400	2/26	60.78	2.2 ± 0.5	6.1 ± 2.5	35.2 ± 1.4	56.5 ± 4.5
PBN700-2	700	2/26	58.66	9.5 ± 0.4	6.9 ± 0.9	15.0 ± 0.1	68.5 ± 1.4
PBN400-5	400	5/5	57.63	6.2 ± 0.6	7.5 ± 0.6	27.3 ± 0.5	59.0 ± 0.8
PBN700-5	700	5/5	55.71	8.4 ± 1.4	6.4 ± 0.0	11.8 ± 0.9	73.4 ± 0.6
CS400-2	400	2/26	43.28	9.4 ± 0.6	12.0 ± 0.2	49.6 ± 1.0	29.0 ± 0.2
CS700-2	700	2/26	38.27	7.3 ± 0.2	13.4 ± 1.4	66.4 ± 2.2	12.9 ± 0.9
CS400-5	400	5/5	40.29	6.5 ± 0.5	14.3 ± 0.5	39.6 ± 1.3	39.5 ± 2.3
CS700-5	700	5/5	33.40	9.9 ± 1.4	14.7 ± 0.3	50.8 ± 0.2	24.6 ± 1.3
PN400-2	400	2/26	57.95	3.5 ± 0.1	14.3 ± 0.2	39.1 ± 1.6	43.1 ± 1.3
PN700-2	700	2/26	40.12	0.8 ± 0.2	32.4 ± 1.5	10.1 ± 0.2	56.7 ± 1.5
PN400-5	400	5/5	55.96	5.2 ± 1.2	20.3 ± 0.9	19.7 ± 1.5	54.9 ± 0.6
PN700-5	700	5/5	37.57	4.3 ± 0.4	38.9 ± 0.4	8.3 ± 1.6	48.5 ± 2.4
CM400-2	400	2/26	52.98	3.9 ± 0.1	40.7 ± 0.8	28.6 ± 0.7	26.7 ± 0.0
CM700-2	700	2/26	47.25	2.4 ± 0.0	50.3 ± 0.1	9.9 ± 0.3	37.3 ± 0.2
CM400-5	400	5/5	48.41	3.3 ± 0.2	37.2 ± 1.5	19.7 ± 0.5	39.8 ± 1.3
CM700-5	700	5/5	44.66	3.8 ± 1.4	37.8 ± 0.5	8.0 ± 2.5	50.5 ± 4.4
CYMB400-2	400	2/26	40.61	5.8 ± 0.0	6.6 ± 0.1	40.0 ± 0.3	47.5 ± 0.2
CYMB700-2	700	2/26	31.78	7.2 ± 0.8	9.3 ± 0.1	23.7 ± 1.9	59.8 ± 2.8
CYMB400-5	400	5/5	34.70	4.8 ± 0.9	6.3 ± 0.1	18.6 ± 0.1	70.3 ± 0.9
CYMB700-5	700	5/5	26.14	5.9 ± 0.6	9.4 ± 2.0	12.8 ± 0.1	71.9 ± 1.5

[a]*Mean values (n = 3) with S.D.*

conditions. Pyrolysis of CYMB700-5 biomass resulted in only 26.1% biochar yield, which was considerably low when compared to more organic-rich biomass, such as cow manure and corn stover. These findings suggested that CYMB biomass had a more condensed structural matrix and a more reactive surface prone to extended volatilization (**Table 1**). We have found that volatile matter diminished with the increase of pyrolytic temperature, which was confirmed by several studies on other types of biomass (Sharypov et al., 2002; Novak et al., 2009; Enders et al., 2012; Noor et al., 2012; Angin, 2013; Sadaka et al., 2014).

The chosen interval of residence time could affect the necessary reaction time during the re-polymerization of the biochar's structure. Long residence time could promote a formation of condensed aromatic structures with an abundance of micro-, meso- and macropores, producing a higher yield of fixed carbon and enhanced porosity (Tripathi et al., 2016). The development of more stable aromatic structures is due to the cleaving of volatile parts of the biomass during prolonged thermal treatment (Tripathi et al., 2016; Wang et al., 2019).

The yields of fixed carbon for all produced biochar are summarized in **Table 1**. The comparison of obtained results has confirmed the link between time/temperature of pyrolysis and yield of fixed carbon; however, the specific concentration in tested biochar depended on the kind of starting biomass. It was interesting to observe the unique impact of high potassium content determined in corn stover (CS) on the efficacy of volatilization. Obtained results for corn stover (CS) biochar could be explained through extremely high loads and catalytic effect of potassium (K) (ranged 58.4–71.9 g kg^{-1}) when compared to all other types of biochar produced (ranged 0.1–9.0 g kg^{-1}). It is well known that alkali metals in biomass have a substantial influence on the thermal degradation (Fahmi et al., 2007), where potassium acts as a catalyst during pyrolytic reactions (Nowakowski et al., 2007; Nowakowski and Jones, 2008). Only a small amount of potassium (<10%) is bound to hydroxyl or carboxyl groups in cellulose and hemicellulose of biomass (Saddawi et al., 2012). During their thermal degradation at lower temperatures (<400°C), some potassium can potentially be released in the gas phase (Akbar et al., 2010). On the contrary, the greater amount of K integrated into the biochar matrix, will undergo further reactions at higher pyrolytic temperatures (Nowakowski et al., 2007). As pyrolytic temperature increases, the water-insoluble K thereafter progresses to form K_2CO_3 > K_2O > K_2O_2 (Shen et al., 2015; Chen et al., 2017; Xiao et al., 2018), where the reducing (K_2O-C) and oxidizing (K_2O_2-C) forms of the K-C-O intercalates, act as catalysts in biochar gasification (Wang et al., 2010). This suggests that CS biochar produced at 700°C is potentially abundant in alkali metal salts, contrary to CS biochar produced at 400°C containing more readily gasified organic products. When samples are heated at 950°C to determine the loss of readily volatilized compounds, CS400 biochar could account volatile loss greatly due to volatiles such as alcohols, acids, etc., while CS700 biochar could attribute an increase in volatile loss to high K content, rapidly volatilizing at 950°C into the gas phase (Van Lith et al., 2008; Chen et al., 2017).

Considering that the increased availability of surface-bonded potassium promotes polymerization reactions via rapid ionic

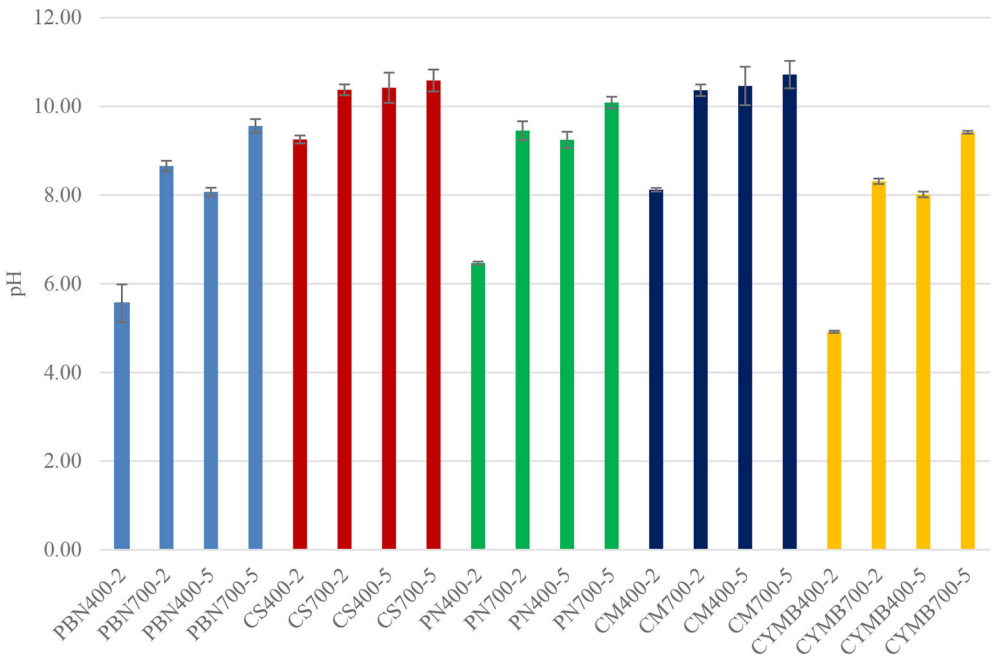

FIGURE 1 | pH of biochar produced at 400 and 700°C for 2 and 5 h. Each kind of biochar is marked with one color (pine bark = blue, corn stover = red, pine needles = green, cow manure = dark blue, cypress mulch = yellow).

mechanisms (Saddawi et al., 2012), results in this study suggest volatile increase with the increase of pyrolytic temperature due to rapid thermal conversion of K_2O and K_2O_2 into the gas phase (H_2, H_2O) (Wang et al., 2010) and their catalytic effect on char formation. Also, results from this study show greater release of water-soluble K^+ for CS biochar produced at 700°C (58.4–71.9 g kg-1), suggesting evolution during pyrolysis by generating new active sites via diffusion of K^+ from salts to chelation complexes (Saddawi et al., 2012).

On the contrary, other studies (Mullen et al., 2010; Rafiq et al., 2016) also reported a significantly lower concentration of K in corn stover biochar, which potentially reduces its catalytic effect to such extent. Since proximate analysis requires quantitative determination under extremely high temperatures (volatile matter at 950°C and ash at 750°C) for prolonged periods, practical drawbacks may result in increased and/or decreased estimates (Enders et al., 2012).

Summarizing, we have recorded that for the CS biochar (rich in mineral content, especially potassium), an increase of temperature from 400 to 700°C, caused the increase of the volatile matter from 49.6 to 66.4% (2 h) and 39.6 to 50.8% (5 h). The volatilization's yield of other types of biochar with minimal contents of potassium (0.4–6.2 g kg^{-1} K) was not impacted.

Results from the study aiming links between biomass and temperature of pyrolysis on produced ash are summarized in **Table 1**. Cow manure (CM) made biochar (CM700-2) produced at 700°C for 2 h resulted in the highest ash content (50.3 %), while under the same pyrolysis conditions, pine bark nuggets biochar (PBN700-2) produced only 6.9 % of total ash. It was noted that ash formation was proportional to the level of nutrients and minerals in starting biomass, as a low ash content was obtained from woody-type biochar only, namely pine bark nuggets (PBN) and cypress mulch blend (CYMB). Also, the longer residence time (5 h) and lower heating rate (5°C/min) notably enhanced char formation by preventing incomplete de-polymerization at high heating rates. Published studies show that the high heating rate promotes secondary pyrolysis at temperatures above 500°C retarding aromatization by further decomposition and volatilization of primary products of pyrolysis (tar, char, ash, CO, CO_2, H_2O, etc.; Lewis and Fletcher, 2013; Amini et al., 2019).

Biochar pH and EC

Earlier studies by Lehmann et al. (2011), Mukherjee et al. (2011), and Yuan et al. (2011) have reported an increase of biochar pH with the increase of pyrolytic temperature and residence time. This trend could be related to the high content of inorganic minerals (K, Ca, Mg, etc.) and the formation of different inorganic alkalis and carbonate salts, such as KOH, $MgCO_3$, $CaCO_3$, etc. resistant to the volatilization at higher temperatures (Cheah et al., 2014; Rehrah et al., 2014). Conversely, biochar produced at lower temperatures tends to be more acidic due to incomplete degradation and conservation of acidic functional groups (Qi et al., 2017). Biochar produced from organic-rich biomass is expected to have a higher content of nutrients, and with the increase of pyrolytic temperature (700–800°C), the preferential decomposition of Ca- and K-bonded components of biomass would influence final pH (Knoepp et al., 2005).

Figure 1 provides a comparison of the variation of pH depending on pre-set conditions of pyrolysis. We have found

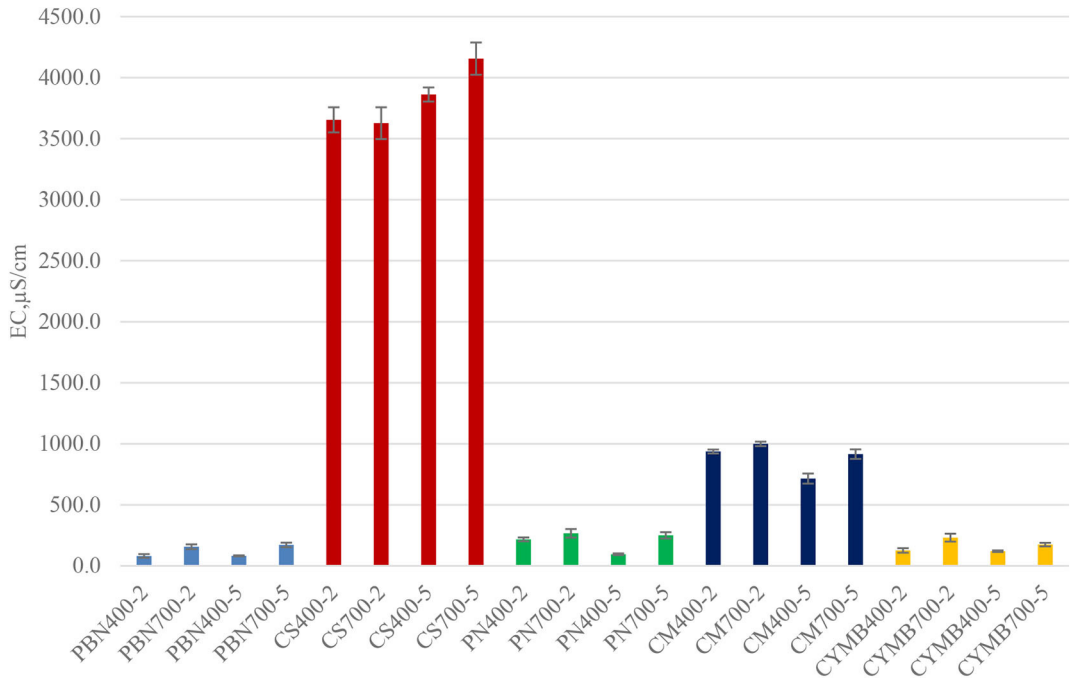

FIGURE 2 | Conductivity (EC) of biochar produced under different initial conditions (400 and 700°C; 2 and 5 h).

that corn stover (CS) and cow manure (CM) based biochar had the highest average pH (10.5–10.7) when compared with other types of tested biochar, and the increase of pH was strongly correlated with the temperature of pyrolysis. When the same heating rate and residence time were applied, but the temperature increased from 400 to 700°C, we have recorded a parallel increase of pH by the 1.5–40%. At the same time, cypress mulch(CYMB), pine bark (PBN) and pine needle (PN) made biochar were acidic (pH < 7) when the pyrolytic temperature was 400°C with a shorter residence time of 2 h and higher heating rate (26°C/min).

Current trends in research interest are more focused on the beneficial use of biochar alkalinity; however, the absence of nutrients in acidic biochar shows promising potential in carbon sequestration (87.9%) (Qi et al., 2017). Acidic biochar could be employed to improve the physicochemical properties of calcareous soils (Ippolito et al., 2016).

An interesting correlation was found between pH, conductivity, and concentration of potassium in leachates collected from all tested biochar. As shown in **Figure 2**, biochar made from corn stover (CS) had an unusually high conductivity (3,654–4,155 µS/cm) when compared with other samples. Those values were in a correlation with a high concentration of potassium (58.4–71.9 g kg^{-1} K) (**Table 2**). Expectedly, the woody type of biochar, such as cypress mulch blend (CYMB), had lower pH compared to cow manure (CM) and corn stover (CS) made biochar (**Figure 1**). The lowest recorded pH of 4.92 and conductivity (126.5 µS/cm) was obtained for the cypress mulch blend (CYMB400-2) made biochar. It is important to note that high conductivity was related to the high mineral content of biochar after pyrolysis.

TABLE 2 | Concentrations of biochar nutrients in leachates.

Biochar	Soluble nutrients*				
	Ca, mg/kg^{-1}	K, g/kg^{-1}	Mg, mg/kg^{-1}	P, mg/kg^{-1}	S, mg/kg^{-1}
PBN400-2	125.2	0.4	17.5	–	–
PBN700-2	136.2	0.6	39.6	–	10.4
PBN400-5	111.9	0.1	9.7	–	8.2
PBN700-5	35.2	1.5	13.7	5.4	6.0
CS400-2	37.5	53.6	169.7	1354.9	336.3
CS700-2	14.7	58.4	122.3	2109.7	195.8
CS400-5	21.6	63.7	138.8	419.4	426.1
CS700-5	56.3	71.9	165.4	905.0	56.3
PN400-2	133.9	6.2	144.3	82.5	33.4
PN700-2	58.0	2.3	96.0	38.2	29.5
PN400-5	126.2	1.2	34.8	15.0	17.2
PN700-5	79.4	3.0	35.8	22.4	10.5
CM400-2	101.6	8.4	143.3	355.3	140.5
CM700-2	210.9	1.9	192.3	60.0	197.8
CM400-5	67.4	9.0	22.6	48.8	19.6
CM700-5	212.0	2.4	36.9	15.5	30.2
CYMB400-2	151.3	0.9	27.8	30.5	26.0
CYMB700-2	196.6	1.0	31.5	10.3	19.9
CYMB400-5	72.2	0.5	18.5	10.6	5.0
CYMB700-5	113.5	1.3	30.5	9.3	6.8

*– Below detection limit. *In DIW (1:20).*

Nutrient Analysis in Biochar Leachate

Table 2 provides a summary of the analysis of nutrients found in leachates collected from manufactured biochar. Similarly to pH and conductivity, the capability of biochar

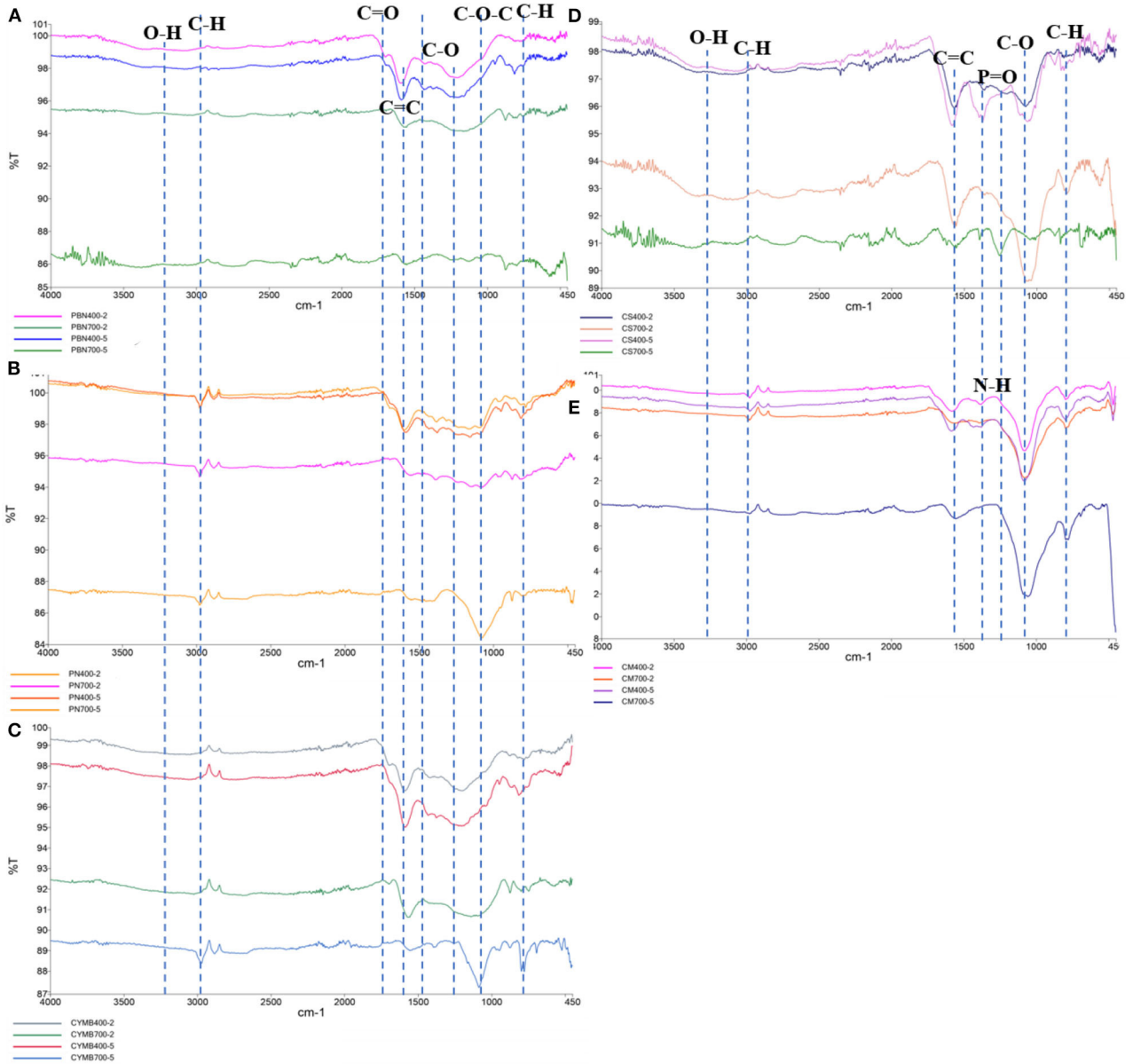

FIGURE 3 | FTIR analysis of functional groups of 20 types of biochar made from **(A)** pine bark, **(B)** pine needle, **(C)** cypress mulch, **(D)** corn stover, **(E)** cow manure.

to exchange cations (CEC) in the water matrix could depend on the biomass's origin. Determined concentrations appeared to be consistent with organic and lignocellulosic fractions in the original biomass. Surprisingly high concentrations of potassium were found not only in corn stover (CS) made biochar, but in all leachates from those samples as well.

The observed trend of potassium content found in leachates was as followed:

$$CS700-5(71.9g/kgK) > CS400-5(63.7g/kgK) > CS400-2(58.4g/kgK) > CS700-2(53.6g/kg\,K)$$

The potassium bonded within the CS biochar was confirmed by the SEM-EDX analysis. Their significant concentrations found in leachates suggested that it was relatively easy to wash potassium from the manufactured biochar, if necessary.

Determination of Functional Groups

Structural and chemical changes, especially availability and abundance of functional groups at the surface of studied biochar, were determined by the Fourier-transform infrared (FTIR) spectroscopy (**Figure 3**). When biochar is produced for a specific application, functional groups of interest are commonly analyzed as a function of biomass source and content, pyrolytic temperature, processing time, and heating rate. These parameters

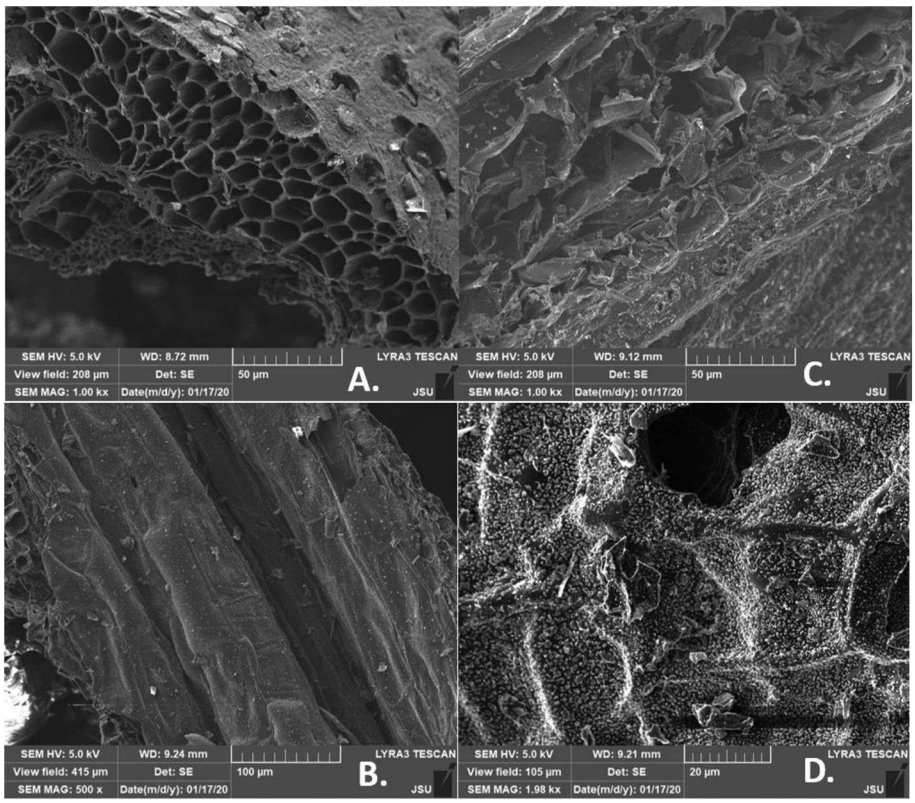

FIGURE 4 | SEM imaging of corn stover (CS) biochar: **(A)** 400°C (5 h, 5°C/min), **(B)** 400°C (2 h, 26°C/min), **(C)** 700°C (2 h, 26°C/min), **(D)** 700°C (5 h, 5°C/min).

have been proven to play a crucial role in assessing biochar's applicability for a particular use (Wang et al., 2018).

Figure 3 contains FTIR spectra of all studied biochar in the following order: (a) pine bark nuggets (PBN), (b) corn stover (CS), (c) pine needles (PN), (d) cow manure (CM), and (e) cypress mulch blend (CMB). It could be seen that obtained spectra were consistent within biochar produced from the same type of biomass but in different pyrolytic conditions. Analysis of all spectra revealed an interesting pattern related to the temperature and residence time of pyrolysis. There were very little or no changes in surface chemistry of biochar produced during 2 or 5 h at 400°C. However, an increase of temperature to 700°C, and extending the time of pyrolysis to 5 h has produced noticeable changes in the occurrence of functional groups and their peak intensities. For example, diminish of existing functional groups (-OH, -COOH, C = O, etc.) with the increase of temperature was observed at the surfaces of pine bark nuggets (PBN), pine needles (PN) and cypress mulch blend (CYMB) made biochar (Mohammed et al., 2018; Muvhiiwa et al., 2019; Liu et al., 2020).

Analysis of a surface of the organic-rich biomass such as corn stover (CS) and cow manure (CM) revealed additional changes. For example, a distinctive P = O bond in the region of 1,209–1,353 cm^{-1} (Wang et al., 2017) was identified for the corn stover. Interestingly, the significantly higher concentration of phosphorus (P) was found in the leachate from this biochar, which suggested substantial loss of this nutrient in the presence of water (**Table 2**). On the other hand, a cow manure (CM) biochar's FTIR spectrum (**Figure 3D**) has confirmed that this particular biochar had the most consistent surface chemistry, and it was the least affected by the temperature and residence time. Also, because of the unique nature of this biomass, the observed presence of amino- group (N-H) between 1,555 and 1,582 cm^{-1} (Qin et al., 2019) was not a surprise. This type of biomass could be employed when N-H groups are needed but required additional treatment of biochar made from other biomasses.

Biochar Morphology and Surface Area

SEM-EDX analysis serves as an essential tool for visual observation of changes occurring on the reactive surface of biochar. The decomposition of hemicellulose, cellulose, and lignin during pyrolysis could explain the increase in surface area and pore size, especially in the woody type of biochar. Hemicellulose degradation usually occurs under 300°C, while the increase of temperature beyond 300°C results in the formation of more amorphous structures during the volatilization (Zhao et al., 2017). The more prolonged exposure to higher temperatures (around 600°C) promotes the formation of more tube-like pores from the degradation of lignin (Zhao et al., 2017; Hyväluoma et al., 2018).

Figure 4 provides SEM images of evolved porosity for corn stover (CS) made biochar produced at 400 and 700°C for either 2 or 5 h. These SEM images support well the theoretical

TABLE 3 | Biochar BET surface areas.

Biochar	Temperature, °C	Residence time, h	BET, m^2/g
PBN400-2	400	2	26.5
PBN700-2	700	2	320.7
CS400-2	400	2	109.1
CS700-2	700	2	72.6
CYMB400-2	400	2	305.9
CYMB400-5	400	5	347.0

explanation provided in previous sections about the catalytic influence of potassium (K) on decreasing fixed carbon content when the higher pyrolytic temperature was applied (700°C). In **Figure 4D**, it could be seen as a visible surface covered with mineral oxides. When biochar obtained from the same type of biomass, but in different initial pyrolytic conditions was compared with other samples, it was evident that higher pyrolytic temperature (700°C) produced a better de-polymerization of charred structures. The ultimate porosity was obtained at 700°C with a heating rate of 5°C/min and a residence time of 5 h.

It is expected that the increase in temperature of pyrolysis would produce a relatively bigger surface area with higher porosity. In our study, the obtained BET values (**Table 3**) have shown that out of all tested samples, the highest surface area (320.67 m^2/g), pore volume (0.15 cm^3/g) and high carbon content (68.5%) was attained by the pine bark nuggets (PBN700-2) made woody biochar. The understanding of the science behind the formation of such structures is essential when the goal is related to the development of large surface areas, similar to activated carbon and carbon nanotubes (Hagemann et al., 2018), which make a carefully manufactured biochar a prime candidate for replacement of more expensive materials.

It should be noted that the pine bark nuggets fired at the lower temperature of 400°C (PBN400-2) produced biochar with a significantly lower surface area (26.52 m^2/g), but with considerably high fixed carbon content >50%). This observation suggested that incomplete structural degradation with reduced porosity occurred due to the limited degradation of lignin at lower pyrolytic temperatures.

When the high nutrient content is found in specific biomass such as corn stover (CS), the proper formation of surface area/porosity would not follow a typical pattern of temperature and residence time. The BET analysis of CS biochar has shown that the CS700-2 biochar had a lower surface area (72.57 m^2/g) compared to CS400-2 (109.10 m^2/g). Such difference could be explained with the higher content of nutrients undergoing the volatilization (**Table 1**).

CONCLUSIONS

Presented research outcomes aimed to correlate biomass sources/content with parameters of pyrolysis and study obtained results, namely physicochemical properties of manufactured biochar. Matrix built on the collected (under the same conditions) results has helped us to understand the possible cross-influences between the content of biomass (high/low mineral/carbon), set up of pyrolysis, and an initial properties of biomass. Biochar is rapidly gaining attention as a potential replacement of more expensive nano-sized carbon used for high-tech applications; therefore, our findings can contribute to a better understanding of correlations between employed biomass and properties of obtained biochar. The examination of all our results allowed concluding the following:

a. The biochar's typical properties, such as carbon content, pH, and surface area, were augmented by the increase of pyrolytic temperature. Conversely, the elevated thermal conditions during biomass' pyrolysis have negatively influenced properties such as yield, volatile matter, and available functional groups.
b. Degradation of cellulose, hemicellulose, and lignin within the same type of biomass is expected to occur under the same reaction rate with similar aromatization patterns. However, results from this work are suggesting a more favorable inclination toward a higher biochar yield in a limited oxygen environment compared to continuous N_2 flow (no oxygen present) reported by other researchers.
c. Corn stover made (CS) biochar produced under a range of different pyrolytic conditions exceeded significantly the typical amount of readily soluble potassium (K), which greatly influenced the increase of pH, EC, and potassium in leachates from this biochar. Potassium-rich type biochar, such as studied corn stover (71.9 g kg^{-1} K), could be a good choice for soil amendment. At the same time, if produced for non-agricultural applications, its catalytic properties could increase surface activity without the additional activation with potassium hydroxide (KOH), as is recommended in many studies.
d. Results from the determination of pH in leachates showed that alkaline-type of biochar ($pH > 7$) could be produced from nutrient-rich biomasses, such as corn stover (CS) and cow manure (CM) at a higher temperature, longer residence time and lower heating rate. Conversely, acidic-type of biochar ($pH < 7$), such as woody cypress mulch bark (CYMB), pine bark nuggets (PBN), or pine needle (PN) made biochar could be produced at lower pyrolytic temperature, shorter residence time and higher heating rate.

Summarizing: not all biomasses are the same. Their values as sustainable material should be carefully evaluated before serving as a source for the custom-made biochar. The same pyrolytic conditions could produce biochar with various properties. In addition, the limited presence of oxygen (instead of pure nitrogen environment) during pyrolysis should be further studied to establish in-depth correlations between parametric deviations and their direct effects on variations of physiochemical properties.

DATA AVAILABILITY STATEMENT

All datasets generated for this study are included in the article/supplementary material.

AUTHOR CONTRIBUTIONS

AU carried out the work. DL provided academic mentoring, supervised the work, and help with preparation of the manuscript. All authors contributed to the article and approved the submitted version.

FUNDING

This work was supported by the National Science Foundation: CREST: HRD-1547754 and EPSCoR R-II: OIA-1632899; and by the U.S. Department of Transportation under Grant Award Number 69A3551747130.

REFERENCES

Ahmad, M., Lee, S. S., Dou, X., Mohan, D., Sung, J.-K., Yang, J. E., and Ok, Y. S. (2012). Effects of pyrolysis temperature on soybean stover- and peanut shell-derived biochar properties and TCE adsorption in water. *Bioresour. Technol.* 118, 536–544. doi: 10.1016/j.biortech.2012.05.042

Ahmad, M., Rajapaksha, A. U., Lim, J. E., Zhang, M., Bolan, N., Mohan, D., et al. (2014). Biochar as a sorbent for contaminant management in soil and water: a review. *Chemosphere* 99, 19–33. doi: 10.1016/j.chemosphere.2013.10.071

Akbar, S., Schnell, U., and Scheffknecht, G. (2010). Modelling potassium release and the effect of potassium chloride on deposition mechanisms for coal and biomass-fired boilers. *Combust Theor Model.* 14, 315–329. doi: 10.1080/13647830.2010.483019

Amini, E., Safdari, M.-S., DeYoung, J. T., Weise, D. R., and Fletcher, T. H. (2019). Characterization of pyrolysis products from slow pyrolysis of live and dead vegetation native to the southern United States. *Fuel* 235, 1475–1491. doi: 10.1016/j.fuel.2018.08.112

Angin, D. (2013). Effect of pyrolysis temperature and heating rate on biochar obtained from pyrolysis of safflower seed press cake. *Bioresour. Technol.* 128, 593–597. doi: 10.1016/j.biortech.2012.10.150

Brunauer, S., Emmett, P. H., and Teller, E. (1938). Adsorption of gases in multimolecular layers. *J. Am. Chem. Soc.* 60, 309–319. doi: 10.1021/ja01269a023

Cao, X., Ma, L., Gao, B., and Harris, W. (2009). Dairy-manure derived biochar effectively sorbs lead and atrazine. *Environ. Sci. Technol.* 43, 3285–3291. doi: 10.1021/es803092k

Cheah, S., Malone, S. C., and Feik, C. J. (2014). Speciation of sulfur in biochar produced from pyrolysis and gasification of oak and corn stover. *Environ. Sci. Technol.* 48, 8474–8480. doi: 10.1021/es500073r

Chen, B., Chen, Z., and Lv, S. (2011). A novel magnetic biochar efficiently sorbs organic pollutants and phosphate. *Bioresour. Technol.* 102, 716–723. doi: 10.1016/j.biortech.2010.08.067

Chen, B., Zhou, D., and Zhu, L. (2008). Transitional adsorption and partition of nonpolar and polar aromatic contaminants by biochars of pine needles with different pyrolytic temperatures. *Environ. Sci. Technol.* 42, 5137–5143. doi: 10.1021/es8002684

Chen, C., Luo, Z., Yu, C., Wang, T., and Zhang, H. (2017). Transformation behavior of potassium during pyrolysis of biomass. *RSC Advances.* 7, 31319–31326. doi: 10.1039/c7ra05162j

Durak, H. (2016). Pyrolysis ofXanthium strumariumin a fixed bed reactor: effects of boron catalysts and pyrolysis parameters on product yields and character. *Energy Sources Part A* 38, 1400–1409. doi: 10.1080/15567036.2014.947446

Durak, H., Genel, S., and Tunç, M. (2019). Pyrolysis of black cumin seed: significance of catalyst and temperature product yields and chromatographic characterization. *J. Liq. Chromatogr. Relat. Technol.* 42, 331–350. doi: 10.1080/10826076.2019.1593194

Enders, A., Hanley, K., Whitman, T., Joseph, S., and Lehmann, J. (2012). Characterization of biochars to evaluate recalcitrance and agronomic performance. *Bioresour. Technol.* 114, 644–653. doi: 10.1016/j.biortech.2012.03.022

Fahmi, A. H., Samsuri, A. W., Jol, H., and Singh, D. (2018). Physical modification of biochar to expose the inner pores and their functional groups to enhance lead adsorption. *RSC Adv.* 8, 38270–38280. doi: 10.1039/C8RA06867D

Fahmi, R., Bridgwater, A. V., Darvell, L. I., Jones, J. M., Yates, N., Thain, S., et al. (2007). The effect of alkali metals on combustion and pyrolysis of Lolium and Festuca grasses, switchgrass and willow. *Fuel.* 86, 1560–1569. doi: 10.1016/j.fuel.2006.11.030

Gabhi, R. S., Kirk, D. W., and Jia, C. Q. (2017). Preliminary investigation of electrical conductivity of monolithic biochar. *Carbon* 116, 435–442. doi: 10.1016/j.carbon.2017.01.069

Gai, X., Wang, H., Liu, J., Zhai, L., Liu, S., Ren, T., et al. (2014). Effects of Feedstock and Pyrolysis Temperature on Biochar Adsorption of Ammonium and Nitrate. *PLoS ONE* 9:e113888. doi: 10.1371/journal.pone.0113888

Hagemann, N., Spokas, K., Schmidt, H.-P., Kägi, R., Böhler, M., and Bucheli, T. (2018). Activated carbon, biochar, and charcoal: linkages and synergies across pyrogenic carbon's ABCs. *Water* 10:182. doi: 10.3390/w10020182

Harvey, O. R., Herbert, B. E., Kuo, L.-J., and Louchouarn, P. (2012). Generalized two-dimensional perturbation correlation infrared spectroscopy reveals mechanisms for the development of surface charge and recalcitrance in plant-derived biochars. *Environ. Sci. Technol.* 46, 10641–10650. doi: 10.1021/es302971d

Hyväluoma, J., Kulju, S., Hannula, M., Wikberg, H., Källi, A., and Rasa, K. (2018). Quantitative characterization of the pore structure of several biochars with 3D imaging. *Environ. Sci. Pollut. Res.* 25, 25648–25658. doi: 10.1007/s11356-017-8823-x

Ippolito, J. A., Ducey, T. F., Cantrell, K. B., Novak, J. M., and Lentz, R. D. (2016). Designer, acidic biochar influences calcareous soil characteristics. *Chemosphere* 142, 184–191. doi: 10.1016/j.chemosphere.2015.05.092

Kastner, J. R., Miller, J., Geller, D. P., Locklin, J., Keith, L. H., and Johnson, T. (2012). Catalytic esterification of fatty acids using solid acid catalysts generated from biochar and activated carbon. *Catalysis Today* 190, 122–132. doi: 10.1016/j.cattod.2012.02.006

Kawamoto, H. (2017). Lignin pyrolysis reactions. *J. Wood Sci.* 63, 117–132. doi: 10.1007/s10086-016-1606-z

Kawamoto, H., Murayama, M., and Saka, S. (2003). Pyrolysis behavior of levoglucosan as an intermediate in cellulose pyrolysis: polymerization into polysaccharide as a key reaction to carbonized product formation. *J. Wood Sci.* 49, 469–473. doi: 10.1007/s10086-002-0487-5

Knoepp, J. D., Neary, D. G.; Ryan, K. C., DeBano, L. F. (eds.). (2005). "Wildland fire in ecosystems: effects of fire on soils and water," in *Gen. Tech. Rep. RMRS-GTR-42-vol.4.* Ogden, UT: U.S. Department of Agriculture, Forest Service, Rocky Mountain Research Station.

Lehmann, J., Rillig, M. C., Thies, J., Masiello, C. A., Hockaday, W. C., and Crowley, D. (2011). Biochar effects on soil biota – A review. *Soil Biol. Biochem.* 43, 1812–1836. doi: 10.1016/j.soilbio.2011.04.022

Lewis, A. D., and Fletcher, T. H. (2013). Prediction of sawdust pyrolysis yields from a flat-flame burner using the CPD model. *Energy Fuels* 27, 942–953. doi: 10.1021/ef3018783

Liu, N., Zhang, Y., Xu, C., Liu, P., Lv, J., Liu, Y. Y., et al. (2020). Removal mechanisms of aqueous Cr(VI) using apple wood biochar: a spectroscopic study. *J. Hazard. Mater.* 384:121371. doi: 10.1016/j.jhazmat.2019.121371

Lu, H., Zhang, W., Yang, Y., Huang, X., Wang, S., and Qiu, R. (2012). Relative distribution of Pb2+ sorption mechanisms by sludge-derived biochar. *Water Res.* 46, 854–862. doi: 10.1016/j.watres.2011.11.058

Lv, G., and Wu, S. (2012). Analytical pyrolysis studies of corn stalk and its three main components by TG-MS and Py-GC/MS. *J. Anal. Appl. Pyrol.* 97, 11–18. doi: 10.1016/j.jaap.2012.04.010

Mayes, H. B., and Broadbelt, L. J. (2012). Unraveling the reactions that unravel cellulose. *J. Phys. Chem. A* 116, 7098–7106. doi: 10.1021/jp300405x

Mohammed, N. A. S., Abu-Zurayk, R. A., Hamadneh, I., and Al-Dujaili, A. H. (2018). Phenol adsorption on biochar prepared from the pine fruit shells: equilibrium, kinetics, and thermodynamics studies. *J. Environ. Manage* 226, 377–385. doi: 10.1016/j.jenvman.2018.08.033

Mohan, D., Sarswat, A., Ok, Y. S., and Pittman, C. U. (2014). Organic and inorganic contaminants removal from water with biochar, a renewable, low cost and sustainable adsorbent – A critical review. *Bioresour. Technol.* 160, 191–202. doi: 10.1016/j.biortech.2014.01.120

Mohanty, S. K., Valenca, R., Berger, A. W., Yu, I. K. M., Xiong, X., Saunders, T. M., et al. (2018). Plenty of room for carbon on the ground: potential applications of biochar for stormwater treatment. *Sci. Total Environ.* 625, 1644–1658. doi: 10.1016/j.scitotenv.2018.01.037

Mukherjee, A., Zimmerman, A. R., and Harris, W. (2011). Surface chemistry variations among a series of laboratory-produced biochars. *Geoderma* 163, 247–255. doi: 10.1016/j.geoderma.2011.04.021

Mullen, C. A., Boateng, A. A., Goldberg, N. M., Lima, I. M., Laird, D. A., and Hicks, K. B. (2010). Bio-oil and bio-char production from corn cobs and stover by fast pyrolysis. *Biomass Bioenerg.* 34, 67–74. doi: 10.1016/j.biombioe.2009.09.012

Muvhiiwa, R., Kuvarega, A., Maphla, E., and Muleja, A. (2019). Study of biochar from pyrolysis and gasification of wood pellets in a nitrogen plasma reactor for the design of biomass processes. *J. Environ. Chem. Eng.* 7:103391. doi: 10.1016/j.jece.2019.103391

Narzari, R., Bordoloi, N., Sarma, B., Gogoi, L., Gogoi, N., Borkotoki, B., et al. (2017). Fabrication of biochars obtained from the valorization of biowaste and evaluation of its physicochemical properties. *Bioresour. Technol.* 242, 324–328. doi: 10.1016/j.biortech.2017.04.050

Ngan, A., Jia, C. Q., and Tong, S.-T. (2019). Production, characterization and alternative applications of biochar. *Biofuels Biorefineries.* 9, 117–151. doi: 10.1007/978-981-13-3768-0_5

Noor, N. M., Shariff, A., and Abdullah, N. (2012). Slow Pyrolysis of Cassava Wastes for Biochar Production and Characterization. *Iranian J. Energy Environ.* 3, 60–65. doi: 10.5829/idosi.ijee.2012.03.05.10

Novak, J. M., Busscher, W. J., Laird, D. L., Ahmedna, M., Watts, D. W., and Niandou, M. A. S. (2009). Impact of biochar amendment on fertility of a southeastern coastal plain soil. *Soil Sci.* 174, 105–112. doi: 10.1097/SS.0b013e3181981d9a

Nowakowski, D., Jones, J., Brydson, R., and Ross, A. (2007). Potassium catalysis in the pyrolysis behaviour of short rotation willow coppice. *Fuel.* 86, 2389–2402. doi: 10.1016/j.fuel.2007.01.026

Nowakowski, D. J., and Jones, J. M. (2008). Uncatalysed and potassium-catalysed pyrolysis of the cell-wall constituents of biomass and their model compounds. *J. Anal. Appl. Pyrolysis.* 83, 12–25. doi: 10.1016/j.jaap.2008.05.007

Park, J.-H., Wang, J. J., Kim, S.-H., Kang, S.-W., Yoon Jeong, C., Jeon, J.-R., et al. (2019). Cadmium adsorption characteristics of biochars derived using various pine tree residues and pyrolysis temperatures. *J. Colloid Interface Sci.*. 553, 298–307. doi: 10.1016/j.jcis.2019.06.032

Patwardhan, P. R., Brown, R. C., and Shanks, B. H. (2011). Product distribution from the fast pyrolysis of hemicellulose. *Chem. Sus Chem.* 4, 636–643. doi: 10.1002/cssc.201000425

Qi, F., Dong, Z., Lamb, D., Naidu, R., Bolan, N. S., Ok, Y. S., et al. (2017). Effects of acidic and neutral biochars on properties and cadmium retention of soils. *Chemosphere* 180, 564–573. doi: 10.1016/j.chemosphere.2017.04.014

Qin, J., Qian, S., Chen, Q., Chen, L., Yan, L., and Shen, G. (2019). Cow manure-derived biochar: its catalytic properties and influential factors. *J. Hazard. Mater.* 371, 381–388. doi: 10.1016/j.jhazmat.2019.03.024

Rafiq, M. K., Bachmann, R. T., Rafiq, M. T., Shang, Z., Joseph, S., and Long, R. (2016). Influence of pyrolysis temperature on physico-chemical properties of corn stover (Zea mays L.) biochar and feasibility for carbon capture and energy balance. *PLOS ONE.* 11:e0156894. doi: 10.1371/journal.pone.0156894

Rajapaksha, A. U., Chen, S. S., Tsang, D. C. W., Zhang, M., Vithanage, M., Mandal, S., et al. (2016). Engineered/designer biochar for contaminant removal/immobilization from soil and water: potential and implication of biochar modification. *Chemosphere* 148, 276–291. doi: 10.1016/j.chemosphere.2016.01.043

Rehrah, D., Reddy, M. R., Novak, J. M., Bansode, R. R., Schimmel, K. A., Yu, J., et al. (2014). Production and characterization of biochars from agricultural by-products for use in soil quality enhancement. *J. Anal. Appl. Pyrolysis* 108, 301–309. doi: 10.1016/j.jaap.2014.03.008

Sadaka, S., Sharara, M., Ashworth, A., Keyser, P., Allen, F., and Wright, A. (2014). Characterization of biochar from switchgrass carbonization. *Energies* 7, 548–567. doi: 10.3390/en7020548

Saddawi, A., Jones, J. M., and Williams, A. (2012). Influence of alkali metals on the kinetics of the thermal decomposition of biomass. *Fuel Process. Technol.* 104, 189–197. doi: 10.1016/j.fuproc.2012.05.014

Sharypov, V. I., Marin, N., Beregovtsova, N. G., Baryshnikov, S. V., Kuznetsov, B. N., Cebolla, V. L., et al. (2002). Co-pyrolysis of wood biomass and synthetic polymer mixtures. Part I: influence of experimental conditions on the evolution of solids, liquids, and gases. *J. Analyt. Appl. Pyroly.* 64, 15–28. doi: 10.1016/S0165-2370(01)00167-X

Shen, Y., Linville, J. L., Urgun-Demirtas, M., Schoene, R. P., and Snyder, S. W. (2015). Producing pipeline-quality biomethane via anaerobic digestion of sludge amended with corn stover biochar with in-situ CO_2 removal. *Appl. Energy* 158, 300–309. doi: 10.1016/j.apenergy.2015.08.016

Singh, B., Camps-Arbestain, M., and Lehmann, J. (2017). *Biochar: A Guide to Analytical Methods*. Boca Raton: CRC Press.

Suliman, W., Harsh, J. B., Fortuna, A.-M., Garcia-Pérez, M., and Abu-Lail, N. I. (2017). Quantitative effects of biochar oxidation and pyrolysis temperature on the transport of pathogenic and nonpathogenic Escherichia coli in biochar-amended sand columns. *Environ. Sci. Technol.* 51, 5071–5081. doi: 10.1021/acs.est.6b04535

Tripathi, M., Sahu, J. N., and Ganesan, P. (2016). Effect of process parameters on the production of biochar from biomass waste through pyrolysis: a review. *Renew. Sustain. Energy Rev.* 55, 467–481. doi: 10.1016/j.rser.2015.10.122

Uchimiya, M., Wartelle, L. H., Klasson, K. T., Fortier, C. A., and Lima, I. M. (2011). Influence of pyrolysis temperature on biochar property and function as a heavy metal sorbent in soil. *J. Agric. Food Chem.* 59, 2501–2510. doi: 10.1021/jf104206c

Van Lith, S. C., Jensen, P. A., Frandsen, F. J., and Glarborg, P. (2008). Release to the Gas Phase of Inorganic Elements during Wood Combustion. Part 2: Influence of Fuel Composition. *Energ. Fuel.* 22, 1598–1609. doi: 10.1021/ef060613i

Wang, D., Zhang, W., Hao, X., and Zhou, D. (2013). Transport of biochar particles in saturated granular media: effects of pyrolysis temperature and particle size. *Environ. Sci. Technol.* 47, 821–828. doi: 10.1021/es303794d

Wang, J., Yao, Y., Cao, J., and Jiang, M. (2010). Enhanced catalysis of K_2CO_3 for steam gasification of coal char by using $Ca(OH)_2$ in char preparation. *Fuel.* 89, 310–317. doi: 10.1016/j.fuel.2009.09.001

Wang, M., Zhu, Y., Cheng, L., Andserson, B., Zhao, X., Wang, D., et al. (2018). Review on the utilization of biochar for metal-contaminated soil and sediment remediation. *J. Environ. Sci.* 63, 156–173. doi: 10.1016/j.jes.2017.08.004

Wang, S., Guo, W., Gao, F., and Yang, R. (2017). Characterization and Pb(II) removal potential of corn straw- and municipal sludge-derived biochars. *Royal Soc. Open Sci.* 4:170402. doi: 10.1098/rsos.170402

Wang, Z., Liu, K., Xie, L., Zhu, H., Ji, S., Shu, X., et al. (2019). Effects of residence time on characteristics of biochars prepared via co-pyrolysis of sewage sludge and cotton stalks. *J. Anal. Appl. Pyrolysis.* 142, 104659. doi: 10.1016/j.jaap.2019.104659

Xiao, X., Chen, B., Chen, Z., Zhu, L., and Schnoor, J. L. (2018). Insight into multiple and multilevel structures of biochars and their potential environmental applications: a critical review. *Environ. Sci. Technol.* 52, 5027–5047. doi: 10.1021/acs.est.7b06487

Xue, Y., Gao, B., Yao, Y., Inyang, M., Zhang, M., Zimmerman, A. R., et al. (2012). Hydrogen peroxide modification enhances the ability of biochar (hydrochar) produced from hydrothermal carbonization of peanut hull to remove aqueous heavy metals: batch and column tests. *Chem. Eng. J.* 200–202, 673–680. doi: 10.1016/j.cej.2012.06.116

Yan, J., Han, L., Gao, W., Xue, S., and Chen, M. (2015). Biochar supported nanoscale zerovalent iron composite used as persulfate activator for removing trichloroethylene. *Bioresour. Technol.* 175, 269–274. doi: 10.1016/j.biortech.2014.10.103

Yang, G.-X., and Jiang, H. (2014). Amino modification of biochar for enhanced adsorption of copper ions from synthetic wastewater. *Water Res.* 48, 396–405. doi: 10.1016/j.watres.2013.09.050

Yorgun, S., and Simşek, Y. E. (2008). Catalytic pyrolysis of Miscanthus×giganteus over activated alumina. *Bioresour. Technol.* 99, 8095–8100. doi: 10.1016/j.biortech.2008.03.036

Yuan, J.-H., Xu, R.-K., and Zhang, H. (2011). The forms of alkalis in the biochar produced from crop residues at different temperatures. *Bioresour. Technol*. 102, 3488–3497. doi: 10.1016/j.biortech.2010.11.018

Zhang, J., Liu, J., and Liu, R. (2015). Effects of pyrolysis temperature and heating time on biochar obtained from the pyrolysis of straw and lignosulfonate. *Bioresour. Technol.* 176, 288–291. doi: 10.1016/j.biortech.2014.11.011

Zhao, S. X., Ta, N., and Wang, X. D. (2017). Effect of temperature on the structural and physicochemical properties of biochar with apple tree branches as feedstock material. *Energies* 10:1293. doi: 10.3390/en10091293

Conflict of Interest: The authors declare that the research was conducted in the absence of any commercial or financial relationships that could be construed as a potential conflict of interest.